

Leon X-1, the first *Chandra* Source.¹

Martin C. Weisskopf¹, Tom Aldcroft², Robert A. Cameron², Poshak Gandhi³,
Cedric Foellmi³, Ronald F. Elsner², Sandeep K. Patel⁴, & Stephen L. O'Dell¹

ABSTRACT

Here we present an analysis of the first photons detected with the *Chandra* X-ray Observatory and an identification of the brightest source in the field which we named Leon X-1 to honor the momentous contributions of the *Chandra* Telescope Scientist, Leon Van Speybroeck. The observation took place immediately following the opening of the last door protecting the X-ray telescope. We discuss the unusual operational conditions as the first extra-terrestrial X-ray photons reflected from the telescope onto the ACIS camera. One bright source was apparent to the team at the control center and the small collection of photons that appeared on the monitor were sufficient to indicate that the telescope had survived the launch and was approximately in focus, even prior to any checks and subsequent adjustments.

Subject headings: galaxies:active — history and philosophy of astronomy — X-rays:general

1. Introduction

After attempts the evenings of July 19 and July 21, the *Chandra* X-ray Observatory was launched on July 23, 1999 using the Space Shuttle *Columbia*. There were, however, several

¹Space Science Department, NASA Marshall Space Flight Center, SD50, Huntsville, AL 35812

²Smithsonian Astrophysical Observatory, Cambridge, MA 02138

³European Southern Observatory, Alonso de Cordova 3107, Vitacura, casilla 19001, Santiago, Chile

⁴USRA, Space Science Department, NASA Marshall Space Flight Center, SD50, Huntsville, AL 35812

¹Based on observations made at the European Southern Observatory, La Silla, Chile

important technical events that took place prior to the initial operation. Separation from the Space Shuttle, firing of the solid rocket Inertial Upper Stage, five firings of the *Chandra* internal engines, and the opening of numerous doors designed to protect the instruments and the telescope from contamination were all necessary. On 1999, August 12, the last door between the X-ray sky and the telescope-detector combination was opened. At this time, the Advanced CCD Imaging Spectrometer (ACIS) was in the focal plane, with the telescope aim point on one of the back-illuminated CCDs, S3. The Observatory had been launched with the idea that this was the best configuration, should the instrument translation assembly not function. The Observatory also provides for focus adjustment, and the detector had been placed at the nominal best focus based on ground calibration.

When the doors opened, the attitude control system was not yet in what was to be the normal operating mode. At this time the aspect camera was taking data, but was not an active part of the attitude control system. The fine attitude of the spacecraft had not yet been established, so that the absolute pointing direction was uncertain by up to 10 degrees. In addition, the dither mode was not yet activated. (The dither mode is used to move the image about a small region in the focal plane to avoid focusing onto a single pixel.) The *Chandra* gyroscopes, which have very small drift, were controlling the spacecraft's attitude.

It is impossible to convey the excitement and tension that preceded the moments when the first photons were detected and displayed on a viewing screen. The *Chandra* Project, which had its formal origins with an unsolicited proposal to NASA in 1976 (Riccardo Giacconi Principal Investigator, Harvey Tananbaum Co-Principal Investigator) was 23 years in the making and the anticipation of the result of this effort was keenly felt by all.

After several minutes it was clear not only that the photons were being detected, but more so, that there was a small cluster of a few photons concentrated within about one arc second, not far from the optical axis. One of us (MCW) dubbed the source Leon X-1 to acknowledge the enormous contribution to the Project by the Telescope Scientist, Leon Van Speybroeck.

Here we present an analysis of the data obtained during this historic observation.

2. Observations and data analysis

The first *Chandra* observation (ObsID 62568) lasted 9-ksec and used ACIS CCDs S2, S3, I0, I1, I2, I3 in the timed-exposure mode with a frame time of 3.241 s.

During the observation, the aspect camera was tracking 6 stars which had been ac-

quired during a full-field search. This observation is unique in that the set of stars was chosen autonomously by the aspect camera, rather than being preselected via ground commanding. Furthermore, the on-board attitude estimate during the observation was offset by approximately 7 degrees from the true attitude. We needed to prepare special input files for a custom run of the aspect data processing pipeline to produce the aspect solution. This solution showed that the Observatory was pointed approximately at $\alpha_{2000} = 5^{\text{h}} 19^{\text{m}} 34^{\text{s}}$ and $\delta_{2000} = -60^{\circ} 43' 11''$. However, there is an uncertainty of several arcseconds because the observation was done without tracking the aspect fiducial lights, which allow precise registration of the science instrument focal plane relative to the telescope boresight. In Section 2.1 we circumvent this limitation by fine tuning the aspect solution using detected X-ray sources.

Chandra X-ray Center (CXC) processing (CXCDs 6.2.4) was used to create Level 2 event lists. Events in pulse invariant channels corresponding to 0.5 to 8.0 keV were selected for the purpose of finding sources on the front-illuminated CCDs S2, I0-I3. The energy range 0.25 to 8.0 keV was utilized for source finding with S3. Due to uncertainties in the low energy response, data in the range 0.5 to 8.0 keV were used for spectral analyses. There were no instances of increased background.

2.1. Image Analysis

We used the same source finding techniques as described in Swartz et al. (2003) with the circular-Gaussian approximation to the point spread function, and a minimum signal-to-noise (S/N) ratio of 2.6 resulting in much less than 1 accidental detection in the field. The corresponding background-subtracted point source detection limit is ~ 10 counts which corresponds to a flux (0.5-8.0 keV) of about 7×10^{-15} ergs cm^{-2} s^{-1} for an unabsorbed powerlaw of spectral index -1.5. Fifteen sources were found: one on S2, ten on S3, and four on the I-array. It is not surprising that the majority of the sources were on S3 since this CCD was at the prime focus and has the highest sensitivity of the ACIS CCDs for detecting point sources.

We immediately noticed that there appeared to be a systematic offset of $\approx 5''$ between several of the X-ray sources and potential optical counterparts in the United States Naval Observatory Catalog USNO-B1.0 (Monet et al. 2003 - hereafter USNO-B1.0), one of which was a seventh magnitude guide star. To fine tune the aspect solution, we minimized the separation between the X-ray and optical positions (§ 2.2) using a position-error weighted least squares fit with the right ascension, declination, and roll angle of the pointing position as free parameters. Uncertainties in the optical positions were taken from the USNO-B1 catalog.

The uncertainty in the X-ray position for these calculations was given by $1.51(\sigma^2/N + \sigma_s^2)^{1/2}$ where σ determines the size of the circular Gaussian that approximately matches the point spread function at the source location, N is the aperture-corrected number of source counts, σ_s is a systematic error, and the factor 1.51 is to set the radius that encloses 68% of the circular Gaussian. We allowed δRA , δDec , and $\delta Roll$ to vary freely for different assumed values of σ_s ranging from 0'0 to 0'4. Once the resulting offsets were applied to the X-ray positions, all the fits were excellent independent of the choice for σ_s . Uncertainties in the plate scale² imply a systematic uncertainty of 0'13, and, given that, where relevant, the USNO and 2MASS and CXO positions agree to high precision, we feel that using 0'2 is a reasonable and conservative estimate for σ_s . Considering that we have ignored any possible systematic errors in the non-X-ray positions, such as those due to proper motion, we feel that reducing the value of σ_s is probably unjustified. We note that this choice for σ_s has no statistically significant impact on the positions of the X-ray sources.

Table 1 lists the 15 X-ray sources. The table gives the source positions, the extraction radius, the net counts, the signal-to-noise ratio, and the associated uncertainty in the X-ray position. The brightest X-ray source, S305, is the source Leon X-1. Table 1 also indicates whether or not the source is identified with a potential counterpart in either the USNO-B1.0 or the Two Micron All Sky Survey (2MASS) and lists the angular separation between the X-ray position and the optical/infrared position.

2.2. Optical and Infrared Counterparts

The BROWSE feature³ was used to search for cataloged candidate counterparts centered on the X-ray positions listed in Table 1. All available catalogs were selected to be interrogated. The non-X-ray candidate counterparts were selected by searching a circular region centered on the X-ray position and whose radius was the 99%-confidence radius (3.03/1.51 times the positional uncertainty listed in column 7) continuing the assumption that the point-spread function is described by a circular Gaussian. We do recognize, of course, that the assumption is not perfectly accurate far off-axis, however, this is partially compensated in that there is a good deal of conservatism built into the definition of the positional uncertainty. Of course there is no impact on the coordinates of the X-ray sources.

²see <http://asc.harvard.edu/cal/Hrma/optaxis/platescale/>

³see <http://heasarc.gsfc.nasa.gov/db-perl/W3Browse/w3browse.pl>

2.2.1. USNO-B1.0

The positions of the candidate optical counterpart are listed in Table 2. There are two candidate optical counterparts for I03. There are 2446 USNO-B1.0 sources in a 12' radius centered on the X-ray pointing direction. Thus there are 1.5×10^{-3} sources arcsec⁻² and this density was used to calculate the expected average number of accidental coincidences, N_{r99} , listed in column 4 of Table 2. The probability of getting one or more matches by chance is given by the Poisson probability, $1 - e^{-N_{r99}}$, which for small values of the exponent is approximately N_{r99} . In most cases (9 of 16) these probabilities are below 1%. In two cases (I02, I04), where the probability was higher than 10%, we chose not to search for counterparts. The separation between the X-ray source and the optical source was listed in the 9-th column of Table 1.

The candidate optical counterpart to S310 is a seventh magnitude A3 V star. We note (see also the discussion in § 4) that this star is so bright that it might be hiding other viable counterpart candidates.

2.2.2. 2MASS

We found 3 candidate 2MASS counterparts as listed in Table 2. There are 6427 2MASS sources in the 12' radius circle centered on the pointing position and the inferred density was used to calculate the average number of accidental occurrences accidental listed in column 7 of Table 2. Other pertinent information concerning the potential infrared counterparts is listed in Tables 2 and 3. In Table 2 we have also listed, where relevant, the separation between the optical and the infrared candidate counterparts. In all cases, these separations are subarcsecond implying that there is a good chance that the optical and the infrared sources are the same.

Table 3 gives the magnitudes and colors of the three 2MASS candidate counterparts and Figure 1 show the sources with 2MASS candidate counterparts on a color-color diagram for the field. The 2MASS colors for the A3 V star (Table 3), the counterpart to S310, are consistent with the stellar classification. The other two 2MASS sources, however, do not lie on the main sequence independent of the amount of absorption (reddening), and thus are possibly unobscured AGN. The similarity of the colors of the 2MASS counterparts to S305 (Leon X-1) and S309 would indicate that the two may be similar types of objects.

2.3. Other X-Ray Observations

The BROWSE feature was also used to search for other X-ray observations of the *Chandra* sources. Only various *ROSAT* Catalogs yielded possible coincidences. The faint ($(9.9 \pm 3.9) \times 10^{-3}$ cps) source 1RXS J052145.5-602906 is within about $14''$ of IA04 and the bright ($(6 \pm 1) \times 10^{-2}$ cps) source 1RXS J051934.0-604800 is within $17''$ of Leon X-1. The *ROSAT* positions are sufficiently close enough for us to consider these coincidences as possible prior observations. As discussed below, this implies that Leon X-1 varied significantly between the *ROSAT* and *Chandra* observations.

2.4. Spectral Analysis

Point-source counts and spectra were extracted from within the appropriate radii listed in Table 1. Background was estimated by creating data sets, one each for S2, S3, and the I-array, wherein all data within a region centered on each X-ray source and with a radius of 10 times the extraction radius was removed.

Only the brightest source, Leon X-1, had sufficient counts to warrant a serious spectral analysis. Because the source was far off-axis ($\sim 5'$) the image was sufficiently spread out so that the effects of pileup, estimated to be no more than 5%, could be safely ignored. These data, obtained at the onset of the mission, preceded any damage to the front-illuminated CCDs caused by low-energy protons reflecting from the X-ray telescope onto ACIS during passages through the radiation belts. The ACIS detectors had not yet experienced any passages through the radiation belts with the telescope open to outer space. (We note that the practice of leaving ACIS at the prime focus during belt passages was abandoned once the radiation problem was understood.) Furthermore, there had no build-up of molecular contamination on the ACIS optical-blocking filters.

The spectral analysis used CIAO 3.0.2 to extract the pulse invariant (PI) files and CXC CALDB 2.25 calibration files (gain maps, quantum efficiency uniformity and effective area) to generate the effective area and response functions. The abundances of, and the default cross sections in, TBABS (available in XSPEC ⁴ v.11.2) by Wilms, Allen & McCray (2000) were used in calculating the impact of the interstellar absorption. The data were grouped to assure no less than 15 counts per spectral bin. Except where especially indicated, all errors on spectral parameters are extremes on the two-interesting-parameter, 68%-confidence contours. Spectral analyses were restricted to the energy range 0.5-8.0 keV because of the uncertainties

⁴see <http://heasarc.gsfc.nasa.gov/docs/xanadu/xspec/>

in the ACIS spectral response at low energies.

Three spectral models were applied. The first model, an absorbed powerlaw, led to a statistically acceptable fit (χ^2 of 53.0 for 58 degrees of freedom). The photon index was 2.05 (+0.11, -0.08) and flux was essentially unabsorbed with $0.0 < N_H/10^{22}(cm^{-2}) < 0.026$. The low value for N_H is in line with the value of $4 \times 10^{20}(cm^{-2})$ one infers from radio data using colden.⁵ The flux (0.5-8.0 keV) was 6.8×10^{-13} ergs $cm^{-2} s^{-1}$. The best fit powerlaw spectrum with residuals is shown in Figure 2. Contour plots of $N_H/10^{22}(cm^{-2})$ versus the photon index are shown in Figure 3. We note that the best fit spectrum is what one might expect from a pulsar wind nebula or an AGN.

We also fit the spectrum with a simple blackbody model and the XSPEC model mekal. With the mekal model we set $Z = 1.0Z_\odot$. Both of these fits were unacceptable with χ^2 of 233 and 120 respectively.

Finally, we fit these data with a two-temperature mekal (not unusual for stars). As with the powerlaw, this model also provided a statistically acceptable fit ($\chi^2 = 54$ on 57 degrees of freedom). The best-fit temperatures were 0.25 (+0.04; -0.04) and 4.6 (+1.9; -1.1) keV with the higher temperature component accounting for about 82% of the total flux, hence the absence of lines and the similarity to a thermal bremsstrahlung. The best-fit absorbing column was once again small, $N_H(cm^{-2})/10^{22} = 0.0 (+0.1, -0.0)$. The uncertainties here are the extremes on the 68%-confidence contours but now based on four interesting parameters.

The next brightest source, S310, had only about 160 counts. We grouped the spectral data so as to achieve at least 15 counts per bin and fit to the powerlaw, blackbody and mekal models. The powerlaw fit was statistically unacceptable with $\chi^2 = 10$ on 4 degrees of freedom. Both the blackbody and mekal models yielded acceptable fits but with very different parameters as listed in Table 4. The flux (listed in Table 1) for this source was the same for both spectral models.

For the remaining 13 sources, all with fewer than 100 detected source counts, no spectral fitting was attempted. These sources were, however, included in the X-ray color-color diagrams presented in the following section. We did add together the spectra of the weaker sources on S3 (1-4, 6-9) and fit the summed spectrum to an absorbed powerlaw. This spectrum was scaled by the number of detected counts to establish the flux estimates given in Table 1.

⁵<http://heasarc.gsfc.nasa.gov/cgi-bin/Tools/w3nh/w3nh.pl>

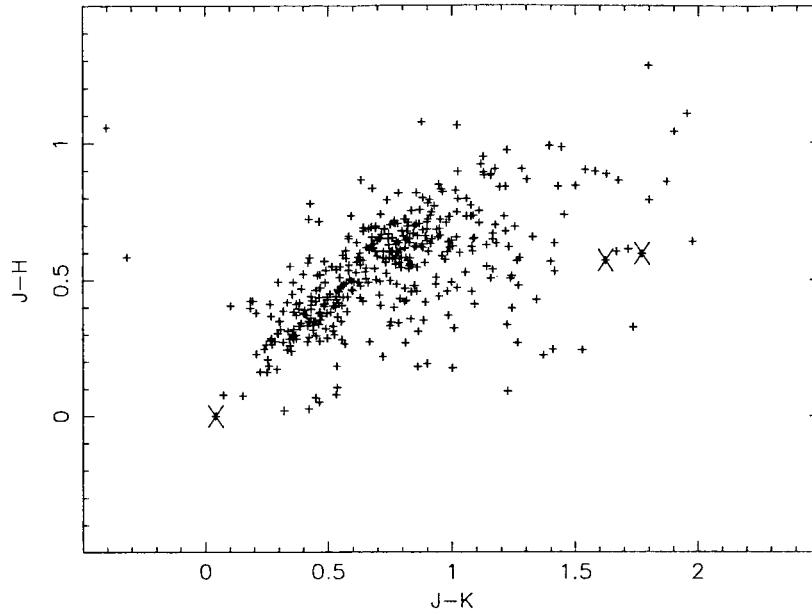


Fig. 1.— Color-color diagram for 2MASS field stars located within a 12' radius from the center of the field of view. The three X-ray sources identified with 2MASS sources (from left to right - S310, S309, Leon X-1) are marked with an "X".

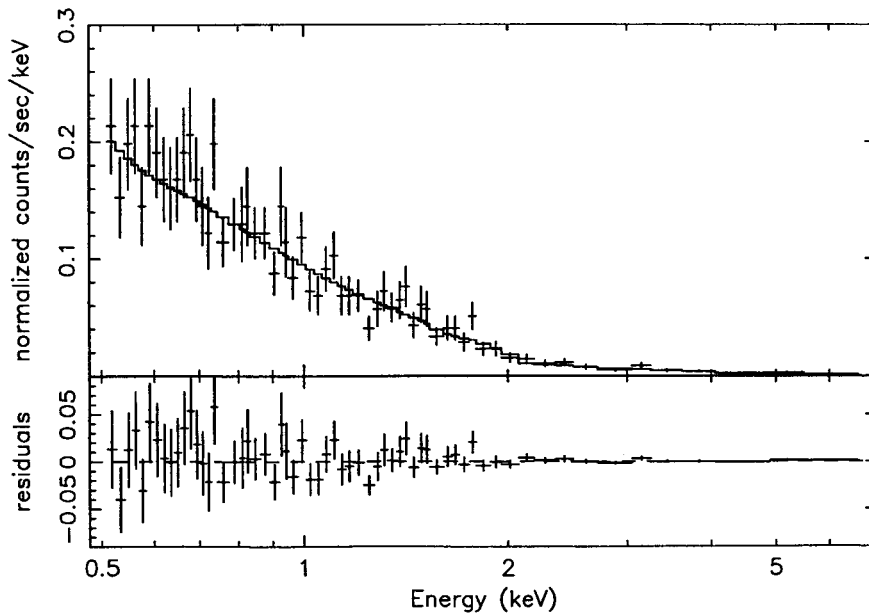


Fig. 2.— The energy spectrum of Leon X-1 fit to an absorbed powerlaw model.

2.4.1. X-ray color-color relation

The bulk of the detected sources were on the back-illuminated CCD, S3, thus we show only the S3 X-ray "color-color" diagram in Figure 4. Since most of the sources were detected with only a small number of counts, the uncertainties are large and it is difficult to draw firm conclusions – see, however, § 4. Thus the diagram is included primarily for completeness. Nevertheless, we note that the hardest source (S302) in the upper-right portion of the diagram has no USNO and/or 2MASS counterpart. It would not be surprising if this turned out to be a heavily obscured AGN. Conversely, the source S310, is the softest source on the diagram as expected based on the spectral analysis presented in § 2.4.

3. Optical Observations

The observations of the optical counterpart to Leon X-1 were carried out with the ESO Multi Mode Instrument (EMMI) imaging-spectrograph at La Silla, Chile, in the morning of Mar 23, 2004. The spectrum is shown in Figure 5. The grism used resulted in a dispersion of 2.86 Å/pix over the observed wavelength range of approximately 3100–9000 Å. Unresolved arc lines were measured to have FWHM ~ 8 Å. The total exposure time was 1800 s and the airmass during the exposure was greater than four.

We find that the spectrum corresponds to a Type 1 (unobscured) AGN, which matches the X-ray spectrum having little/no intrinsic absorption. We also find $z = 0.3207 (\pm 0.0004)$ computed from the variance of the 5 brightest emission lines about the mean) with clear and strong permitted Balmer series emission lines from H α through H ϵ . Forbidden [OIII] $\lambda\lambda$ 4959, 5007 and [OII] $\lambda\lambda$ 3727 Å emission is also seen. The broad lines have full-widths at half-maximum of around 2000–3000 km s $^{-1}$, while the forbidden lines measure ~ 600 km s $^{-1}$. There is slight evidence for a narrow component in the Balmer lines. The detection of broad permitted lines, rising continuum towards the blue (upto ≈ 3500 Å) and measurement of emission line intensity ratios all suggest that Leon X-1 is unreddened in the optical, similar to the unobscured X-ray classification. Note that a flux calibrator could not be observed on the same night, implying some uncertainty in the exact values of the continuum slope and emission line intensity ratios.

4. Discussion & Summary

S305 = Leon X-1 This was the brightest of the first X-ray sources observed with *Chandra*. It was somewhat fortuitous that a source this bright happened to be in the field-of-view. At

a (2.0-8.0 keV) flux level of 1.3×10^{-13} ergs $\text{cm}^{-2} \text{s}^{-1}$, one expects only about 2 such sources per square degree. It was fortunate that the source was sufficiently close to on-axis that its relatively sharply peaked image was easily discernible in the display, thus establishing that the Observatory had survived launch and was operating as expected. We have optically identified this source of magnitude B=17 and determined a redshift of $z = 0.32$. Based on the redshift and the measured spectrum, the luminosity (2.0-8.0 keV) in the rest frame is $\sim 1 \times 10^{44}$ ergs s^{-1} ($H_0 = 70$, $\Lambda_0 = 0.73$). This X-ray luminosity is near the (somewhat arbitrary) dividing line between QSO and Seyfert thus we shall simply identify the source as a Type-1 (unobscured) AGN. We used the spectral data and PIMMS⁶ to determine the *ROSAT* flux and thus establish the inferred variability between the *Chandra* and *ROSAT* observations. We find this variability to be a factor of 9 if we assume that 1RXS J051934.0-604800 is Leon X-1. The inferred variability is even higher if Leon X-1 is not the *ROSAT* source, since then the *ROSAT* data can be used to set an upper limit lower than what was observed. The X-ray variability is also consistent with the AGN classification.

S310 This source is interesting as its optical counterpart appears to be an early main sequence star and its X-ray spectrum is consistent with this conclusion. However, if this is the case, then it is extremely unlikely that the X-rays arise from the counterpart. During the *ROSAT* era, Simon, Drake & Kim (SDK: 1995 and references therein) emphasized that there had been no evidence for X-ray emission from early A-stars and that in those cases where X-ray emission had been detected it was attributed to a companion star. More recently this same point was made by Schmitt (1997). Observations with *Chandra* of the Pleiades open cluster (Daniel, Linsky & Gagne 2002) further support this conclusion. Paraphrasing SDK, the weakness (or absence) of any X-ray emission is a consequence of the effective stellar temperature being too low to drive stellar winds (as for O and early B stars), and too high to achieve envelope convection and thus convectively driven coronae (as for G, K, M stars). Thus we conclude that if the A star is not obscuring another possible counterpart, then the X-ray emission is from a binary companion. One can speculate that the system is not a close binary, in which case the stellar rotation frequency would be high, and hence the X-ray emission would be hard.

S309 Based on its X-ray colors and its 2MASS candidate counterpart, S309 appears similar to S305 (Leon X-1), but note that they possess very different X-ray fluxes.

⁶<http://heasarc.gsfc.nasa.gov/Tools/w3pimms.html>

S303 & S308 Both sources appear, despite large errors, to occupy a distinct and similar part of the X-ray color-color diagram — highly absorbed yet soft. Neither has an USNO or 2MASS candidate counterpart. These may well be obscured AGN.

The other sources Based on the identification of Leon X-1 and its similarities to S309 it is then tempting to argue that all the X-ray sources that occupy a similar region of the X-ray color-color diagram are also unobscured AGN. This conclusion is not unreasonable, based on the large number of AGN observable with *Chandra* (see e.g. Kim et al. 2004).

The first *Chandra* field is very interesting and proves to be a forerunner of things to come. Despite the brief integration time of less than 10 ksec, the first-light observation detected an object which could quite easily turn out to be a highly obscured AGN. Future observations and identifications with objects in other wavelength bands would begin to uncover the highly obscured quasars that many observations with *Chandra* have now determined to make up the previously missing part of the diffuse X-ray background (see e.g. Alexander et al. 2003 and references therein).

MCW acknowledges, with gratitude, conversations with Marshall Joy and Roc Cutri that clarified some of the mysteries of the infrared portion of the spectrum. He also acknowledges support from the *Chandra* Project, and conversations with Gordon Garmire to clarify the events that took place at the time of the first observation. Finally he wishes to acknowledge the important comments of Doug Swartz and Jonathan Grindlay and their encouragement. This publication makes use of data products from the Two Micron All Sky Survey, which is a joint project of the University of Massachusetts and the Infrared Processing and Analysis Center/California Institute of Technology, funded by the National Aeronautics and Space Administration and the National Science Foundation. We all acknowledge the tremendous contribution of Leon Van Speybroeck to the *Chandra* project and to X-ray Astronomy. We dedicate this paper to his memory.

REFERENCES

- Alexander, D. M., Bauer, F. E., Brandt, W. N., Schneider, D. P., Hornschemeier, A. E., Vignali, C., Barger, A. J., Broos, P. S., Cowie, L. L., Garmire, G. P., Townsley, L. K., Bautz, M. W., Chartas, G., & Sargent, W. L. W. 2003, *ApJ*, 126, 539
- Daniel, K.J., Linsky, J.L., & Gagne, M. 2002, *ApJ*. 578, 486
- Kim, D.-W., Wilkes, B.J., Gree, P.J., et al. 2004, *ApJ*, 600, 59

Monet, D .G., et al. 2003, ApJ, 125, 984

Schmitt, J.H.M.M. 1997, A&A, 318, 215

Simon, T., Drake, S.A., & Kim, P.D., 1995, PASP, 107, 1034.

Swartz, D. A., Ghosh, K.K., McCollough, M.L., Pannuti, T.G., Tennant, A.F. & Wu, K.
2003, ApJS, 144, 213

Wilms, J., Allen, A., & McCray, R. 2000, ApJ, 542, 914

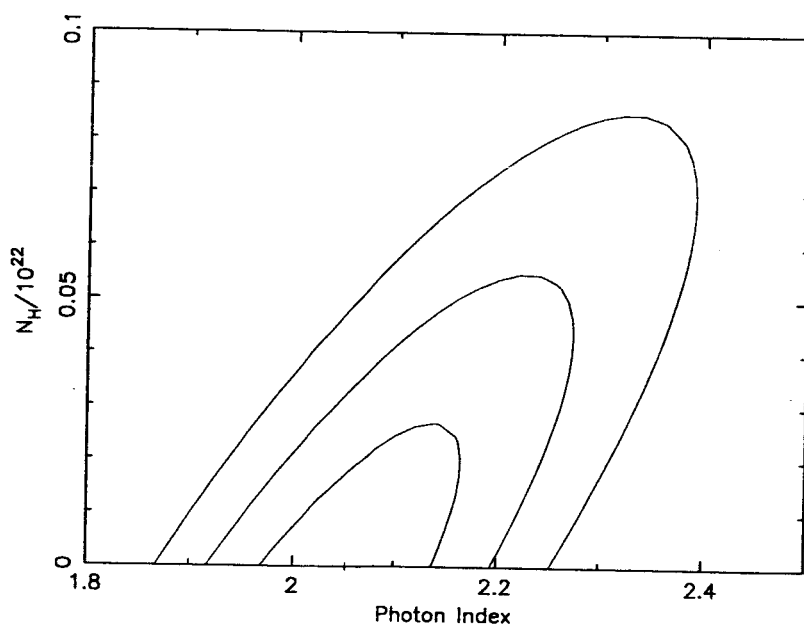


Fig. 3.— Contours of $N_H(cm^{-2})/10^{22}$ versus the powerlaw photon index for Leon X-1. The contours are χ^2 -minimum plus 2.30, 6.17, and 11.8 corresponding to 1-, 2-, and 3- σ for two interesting parameters.

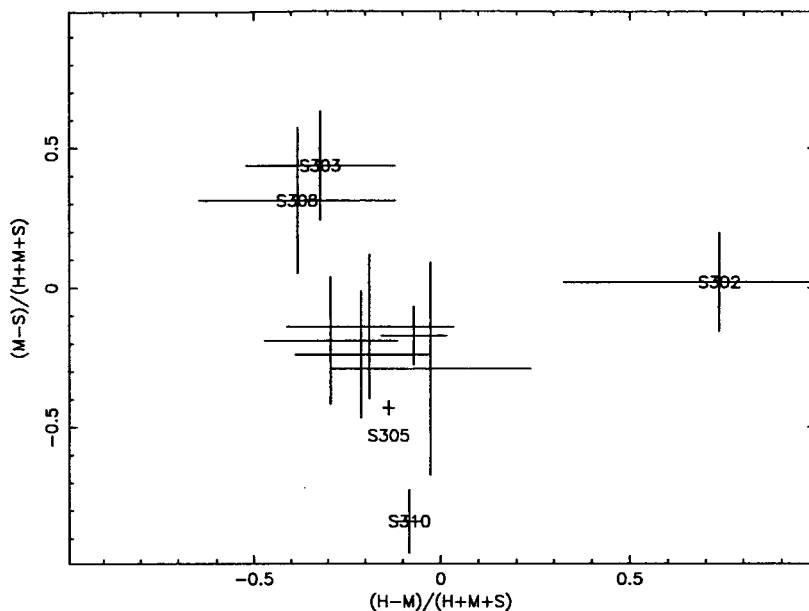


Fig. 4.— X-ray "color-color" diagram for the sources detected with the back-illuminated CCD, S3. The energy bands S, M, and H are defined as follows: S = (0.5 - 1.0) keV, M = (1.0 - 2.0) keV, and H = (2.0 - 8.0) keV. The solid lines are contours for powerlaw spectra of constant photon number index ranging from -1 (innermost) to -4 (outermost) where N_H is varying. The dashed lines are contours of constant N_H for a powerlaw spectrum of varying spectral index. N_H is 0.1, 1, 2, and $5 \times 10^{21} (cm^{-2})$ from the innermost to the outermost contour. Thus a source with spectral index -1 and N_H of $10^{20} (cm^{-2})$ would be placed on the plot at the intersection of the dashed and solid lines at approximately (0.0,0.1).

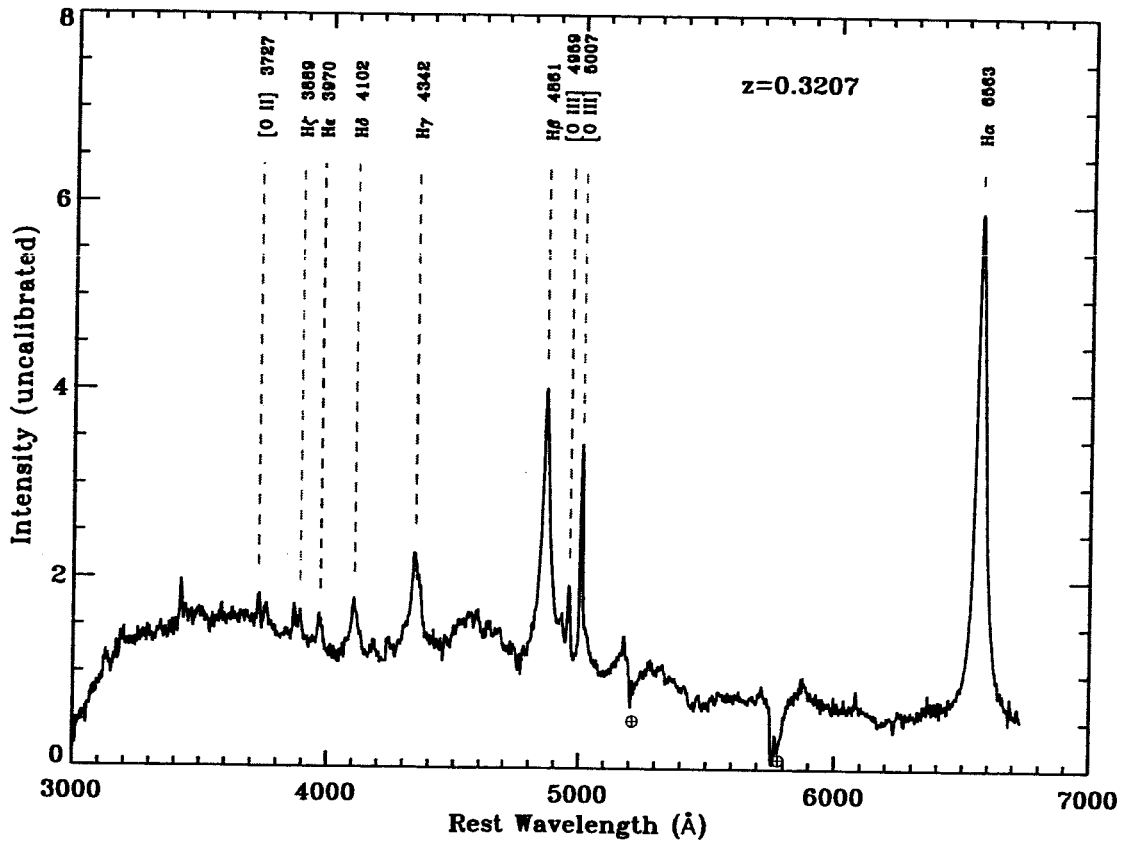


Fig. 5.— ESO EMMI de-reddened spectrum for Leon X-1. The circles with crosses mark the strongest telluric absorption features due to the Earth's atmosphere.

Table 1. X-ray Sources in in the first CXO field in order of increasing RA

NAME	R.A. (J2000)	Dec. (J2000)	r_1^a (")	N^b	S/N^c	r_2^d (")	flux ₁₅ ^e	USNO ^f (")	2MASS ^f (")
S301	79.765785	-60.733794	3.0	8.5	2.8	0.69	6	0.9	
S302	79.779527	-60.750103	2.9	11.0	3.0	0.61	8		
S303	79.800141	-60.733227	2.1	27.7	4.6	0.39	20		
S201	79.824620	-60.554480	1.5	32.2	4.5	1.55	^g	0.4	0.40
S304	79.885861	-60.772111	2.4	21.6	4.5	0.43	15		
S305	79.901102	-60.801187	4.2	1974	41	0.31	6800	0.60	0.5
S306	79.929996	-60.695057	1.5	83.2	7.6	0.32	59	0.40	
S307	79.992341	-60.759039	2.9	22.2	4.5	0.48	16		
S308	79.999462	-60.799583	5.3	17.7	3.8	0.82	13		
S309	80.015201	-60.721160	2.8	16.4	3.8	0.51	12	0.40	0.3
S310	80.117475	-60.779853	8.3	165 7	11	0.49	35	0.10	0.1
I01	80.131245	-60.667099	8.7	15.3	3.2	1.37	^g	1.50	
I02	80.320274	-60.741773	21	19.7	4.3	2.94	^g		
I03	80.320561	-60.683321	22	64.3	6.8	1.68	^g	2.7&1.2	
I04	80.435308	-60.488353	59	94.7	6.9	3.65	^g		

- Note. --
- ^a Source extraction radius
 - ^b Approximate number of source counts
 - ^c Detection Signal-to-Noise ratio
 - ^d X-ray position uncertainty (1σ radius - see discussion in text).
 - ^e This is the (0.5-8.0 keV) flux in units of $\times 10^{-15}$ ergs cm^{-2} s^{-1} .
 - ^f Radial separation between X-ray position and cataloged position of counterpart.
 - ^g See discussion in the text.

Table 2. CANDIDATE COUNTERPARTS TO THE X-RAY SOURCES

NAME	R.A. (J2000) USNO	Dec. (J2000) USNO	N_{r99}^a USNO	R.A. (J2000) 2MASS	Dec. (J2000) 2MASS	N_{r99}^a 2MASS	δ^b (")
s301	79.766284	-60.733748	0.0089			0.0234	
s302			0.0072			0.0189	
s303			0.0029			0.0075	
s201	79.824812	-60.554545	0.0456			0.1197	
s304			0.0035			0.0093	
s305	79.901437	-60.801170	0.0018	79.901378	-60.801132	0.0047	0.17
s306	79.930200	-60.695042	0.0029			0.0077	
s307			0.0044			0.0115	
s308			0.0127			0.0333	
s309	80.015428	-60.721203	0.0050	80.015043	-60.721169	0.0131	0.69
s310	80.117503	-60.779848	0.0046	80.117507	-60.779869	0.0122	0.08
I01	80.132064	-60.666987	0.0359			0.0943	
I02	Not Searched ^c		0.1647	Not Searched ^c		0.4329	
I03	80.320806	-60.683301	0.0534	Not Searched ^c		0.1403	
I03	80.319622	-60.683301	0.0534	Not Searched ^c		0.1403	
I04	Not Searched ^c		0.2537	Not Searched ^c		0.6665	

Note. —

^a The average number of accidental coincidences expected in the region searched.

^b Angular separation between the USNO and 2MASS candidate counterpart.

^c Not searched because of the large value for N_{r99} .

Table 3. 2MASS candidate counterparts: magnitudes and colors

source	J	error	H	error	K _S	error	J-H	error	H-K _S	error	J-K _S	error
S305	16.30	0.12	15.71	0.13	14.53	0.09	0.59	0.17	1.18	0.16	1.77	0.14
S309	16.24	0.14	15.67	0.15	14.61	0.11	0.57	0.20	1.05	0.19	1.62	0.17
S310	6.83	0.02	6.83	0.04	6.79	0.02	0.00	0.05	0.04	0.04	0.04	0.03

Table 4. Spectral Fits to the two brightest sources.

Source	Model	χ^2	ν	$N_H(cm-2)/10^{22}$	Γ or kT
S305	powerlaw	52.9	59	0.0 (0.00 - 0.03)	2.05 (1.97 - 2.16)
S305	mekal	120	59		
S305	bbody	232	59		
S310	powerlaw	10.1	4		
S310	mekal	5.7	4	0.0 (0.00 - 0.37)	0.42 (0.28 - 0.51)
S310	bbody	5.5	4	1.27 (1.09 - 1.45)	0.07 (0.05 - 0.10)

Note. — We do not list values and uncertainties for those fits that are statistically unacceptable.